J|A|C|S
ARTICLES
Published on Web 02/16/2006

PbTe Colloidal Nanocrystals: Synthesis, Characterization, and Multiple Exciton Generation

James E. Murphy,*[,†,§] Matthew C. Beard,[†] Andrew G. Norman,[‡] S. Phillip Ahrenkiel,[†] Justin C. Johnson,[†] Pingrong Yu,[†] Olga I. Mićić,[†] Randy J. Ellingson,[†] and Arthur J. Nozik*[,†,§]

Contribution from the Center for Basic Sciences, the National Center for Photovoltaics, National Renewable Energy Laboratory, Golden, Colorado 80401, and Department of Chemistry and Biochemistry, University of Colorado, Boulder, Colorado 80309

Received November 2, 2005; E-mail: james_murphy@nrel.gov; arthur_nozik@nrel.gov

Abstract: We report an alternative synthesis and the first optical characterization of colloidal PbTe nanocrystals (NCs). We have synthesized spherical PbTe NCs having a size distribution as low as 7%, ranging in diameter from 2.6 to 8.3 nm, with first exciton transitions tuned from 1009 to 2054 nm. The syntheses of colloidal cubic-like PbSe and PbTe NCs using a PbO "one-pot" approach are also reported. The photoluminescence quantum yield of PbTe spherical NCs was measured to be as high as 52 ± 2%. We also report the first known observation of efficient multiple exciton generation (MEG) from single photons absorbed in PbTe NCs. Finally, we report calculated longitudinal and transverse Bohr radii for PbS, PbSe, and PbTe NCs to account for electronic band anisotropy. This is followed by a comparison of the differences in the electronic band structure and optical properties of these lead salts.

Introduction

Due largely to their size-tunable optical properties that result from three-dimensional quantum confinement, colloidal semiconductor nanocrystals (NCs) have been studied extensively for use in a variety of applications. Since the discovery of the quantum confinement effect in lead salt colloids,[1,2] these near- to mid-IR-emitting nanomaterials have been studied for their use in applications such as optoelectronic materials for telecommunications,[3] deep tissue imaging,[4] optical switches,[5] infrared photovoltaics,[4] and photodetectors,[6] as well as thermoelectric applications[7] and electroluminescent devices.[8,9] Recently, a renewed interest in colloidal lead salt quantum dots has arisen due to the experimental confirmation[10,11] of the previously theorized[12,13] process of multiple exciton generation (MEG). Efficient MEG in NCs has the potential to significantly increase the power conversion efficiency of third-generation solar cells employing semiconducting NCs. In contrast to the many well-documented reports on the synthesis and characterization of colloidal PbS[6,8,14−19] and PbSe[20−28] NCs, PbTe[7,29] has received much less attention. This study reports both the synthesis of colloidal PbTe NCs using a one-pot approach and the non-coordinating solvent, 1-octadecene (ODE), as well as the first optical characterization of this material. Specifically, this study reports the first linear absorption spectra, photoluminescence quantum yield (PLQY), and MEG quantum yields of colloidal PbTe NCs.

† Center for Basic Sciences, National Renewable Energy Laboratory.
‡ National Center for Photovoltaics, National Renewable Energy Laboratory.
§ University of Colorado.

(1) Nedeljkovic, J. M.; Nenadovic, M. T.; Micic, O. I.; Nozik, A. J. *J. Phys. Chem.* **1986**, *90*, 12−13.
(2) Nozik, A. J.; Williams, F.; Nenadovic, M. T.; Rajh, T.; Micic, O. I. *J. Phys. Chem.* **1985**, *89*, 397−399.
(3) Harrison, M. T.; Kershaw, S. V.; Burt, M. G.; Rogach, A. L.; Kornowski, A.; Eychmuller, A.; Weller, H. *Pure Appl. Chem.* **2000**, *72*, 295−307.
(4) Sargent, E. H. *Adv. Mater.* **2005**, *17*, 515−522.
(5) Wise, F. W. *Acc. Chem. Res.* **2000**, *33*, 773−780.
(6) McDonald, S. A.; Konstantatos, G.; Zhang, S. G.; Cyr, P. W.; Klem, E. J. D.; Levina, L.; Sargent, E. H. *Nat. Mater.* **2005**, *4*, 138−142.
(7) Lu, W. G.; Fang, J. Y.; Stokes, K. L.; Lin, J. *J. Am. Chem. Soc.* **2004**, *126*, 11798−11799.
(8) Bakueva, L.; Musikhin, S.; Hines, M. A.; Chang, T. W. F.; Tzolov, M.; Scholes, G. D.; Sargent, E. H. *Appl. Phys. Lett.* **2003**, *82*, 2895−2897.
(9) Steckel, J. S.; Coe-Sullivan, S.; Bulovic, V.; Bawendi, M. G. *Adv. Mater.* **2003**, *15*, 1862−1866.
(10) Schaller, R. D.; Klimov, V. I. *Phys. Rev. Lett.* **2004**, *92*, 186601.
(11) Ellingson, R. J.; Beard, M. C.; Johnson, J. C.; Yu, P. R.; Micic, O. I.; Nozik, A. J.; Shabaev, A.; Efros, A. L. *Nano Lett.* **2005**, *5*, 865−871.
(12) Nozik, A. J. *Physica E* **2002**, *14*, 115−120.
(13) Nozik, A. J. *Annu. Rev. Phys. Chem.* **2001**, *52*, 193−231.
(14) Hines, M. A.; Scholes, G. D. *Adv. Mater.* **2003**, *15*, 1844−1849.
(15) Nenadovic, M. T.; Comor, M. I.; Vasic, V.; Micic, O. I. *J. Phys. Chem.* **1990**, *94*, 6390−6396.
(16) Lifshitz, E.; Sirota, M.; Porteanu, H. *J. Cryst. Growth* **1999**, *196*, 126−134.
(17) Klem, E. J. D.; Levina, L.; Sargent, E. H. *Appl. Phys. Lett.* **2005**, *87*, 053101.
(18) Sargent, E. V. H. *J. Mod. Opt.* **2004**, *51*, 2797−2803.
(19) Lee, S. M.; Jun, Y. W.; Cho, S. N.; Cheon, J. *J. Am. Chem. Soc.* **2002**, *124*, 11244−11245.
(20) Murray, C. B.; Sun, S. H.; Gaschler, W.; Doyle, H.; Betley, T. A.; Kagan, C. R. *IBM J. Res. Dev.* **2001**, *45*, 47−56.
(21) Du, H.; Chen, C. L.; Krishnan, R.; Krauss, T. D.; Harbold, J. M.; Wise, F. W.; Thomas, M. G.; Silcox, J. *Nano Lett.* **2002**, *2*, 1321−1324.
(22) Pietryga, J. M.; Schaller, R. D.; Werder, D.; Stewart, M. H.; Klimov, V. I.; Hollingsworth, J. A. *J. Am. Chem. Soc.* **2004**, *126*, 11752−11753.
(23) Wehrenberg, B. L.; Wang, C. J.; Guyot-Sionnest, P. *J. Phys. Chem. B* **2002**, *106*, 10634−10640.
(24) Lifshitz, E.; Bashouti, M.; Kloper, V.; Kigel, A.; Eisen, M. S.; Berger, S. *Nano Lett.* **2003**, *3*, 857−862.
(25) Sashchiuk, A.; Amirav, L.; Bashouti, M.; Krueger, M.; Sivan, U.; Lifshitz, E. *Nano Lett.* **2004**, *4*, 159−165.
(26) Yu, W. W.; Falkner, J. C.; Shih, B. S.; Colvin, V. L. *Chem. Mater.* **2004**, *16*, 3318−3322.
(27) Talapin, D. V.; Murray, C. B. *Science* **2005**, *310*, 86−89.
(28) Brumer, M.; Kigel, A.; Amirav, L.; Sashchiuk, A.; Solomesch, O.; Tessler, N.; Lifshitz, E. *Adv. Funct. Mater.* **2005**, *15*, 1111−1116.
(29) Cho, K. S.; Stokes, K. L.; Murray, C. B. *Abstr. Pap. Am. Chem. Soc.* **2003**, *225*, U74−U75.

PbTe NCs were first synthesized in doped glass by Reynoso et al.[30] in 1995. The synthesis of colloidal PbTe NCs utilizing the organometallic approach[31] was first reported by Cho et al.[29] in 2003 and first published by Lu et al.[7] in 2004. Lu et al. reported on the synthesis of both spherical and cubic-shaped PbTe NCs and state that size-selected precipitation is essential to achieve size distributions of about 7%. We report an alternative route to PbTe NCs derived from cadmium chalcogenide synthetic methods,[32−34] substituting diphenyl ether with the more environmentally friendly solvent ODE, and substituting lead acetate trihydrate with PbO as the initial source of lead for the reaction. We also optimize reaction parameters such as oleic acid/Pb/Te ratios and concentrations and injection and growth temperatures. Furthermore, this one-pot synthesis does not require cooling of the precursors in a glovebox and is therefore more user-friendly. The diameter and size distribution (STD %) of these NCs were measured from TEM images using Digital Micrograph 3.4 software to count a minimum of 100 NCs. The size distribution of these as-synthesized NCs is typically ∼7% for NCs having a first exciton absorption peak at relevant telecommunication wavelengths (1.3−1.6 μm) and as large as 13% for NCs having a first exciton absorption peak around 1 μm.

Experimental Section

Materials. Trioctylphosphine (TOP, technical grade 90%) and myristic acid (98.5%) were purchased from Fluka; 1-octadecene (ODE, technical grade 90%), selenium powder (100 mesh, 99.99%), oleic acid (OA, technical grade 90%), and anhydrous tetrachloroethylene, hexane, methanol, and acetone were purchased from Aldrich; erucic acid (technical grade 85%) and tellurium powder (60 mesh, 99.999%) were purchased from Alfa Aesar.

Synthesis of Spherical Oleate-Capped PbTe Nanocrystals. The synthesis of PbTe nanocrystals was performed in a single, three-neck, round-bottom flask. The lead oleate precursor was prepared by combining PbO with a solution of technical grade oleic acid (OA) and technical grade ODE. The OA/Pb molar ratio ranged between 2.25 for the smallest NCs and 6 for the largest NCs. The lead concentration was diluted to be as low as 0.05 M for the smallest NCs and 0.26 M for the largest NCs using ODE. The mixture was then stirred vigorously while being heated under Ar at 170 °C for about 30 min. The temperature of the resulting transparent solution containing the lead oleate precursor was then adjusted to be between 140 and 170 °C. A stock solution of 0.5 M trioctylphosphine telluride (TOP−Te) was prepared[7] in a glovebox, and a portion, corresponding to a 2:1, Pb/Te ratio (except for the smallest size NCs, see below), was rapidly injected into the reaction vessel. Upon injection, nucleation occurs instantly, so rapid injection is critical to achieve a narrow size distribution. After the injection, the temperature of the reaction vessel was decreased to between 80 and 130 °C and maintained for the remaining growth time. The reaction was quenched by moving the vessel to a cold-water bath and injecting anhydrous hexane equivalent to about 25% of the total reaction volume into the reaction vessel.

A typical synthesis for PbTe NCs having a first excitonic transition between 1500 and 1600 nm involved injecting 1 mL of 0.5 M TOP−Te (0.5 mmol) into a round-bottom flask containing 1 mmol of PbO (0.225 g), 6 mmol of OA (1.89 g of technical grade OA), and 4.7 g of ODE ([Pb] = 0.12 M) at 150 °C. After the injection, the vessel was switched to an oil bath maintained at a temperature of 110 °C. At 6 min the vessel was transferred to a cold-water bath and stirred vigorously as 3 mL of anhydrous hexane was injected into the vessel. As with other lead chalcogenide NCs, PbTe NCs are both air and water sensitive; therefore all postsynthetic treatments were performed in a glovebox with anhydrous reagents. The oleate-capped PbTe NCs were isolated from any remaining starting materials and side products by performing an extraction with methanol, and then precipitating the NCs with acetone. The precipitate was then redissolved in hexane and precipitated again with ethanol. The NCs were redispersed in tetrachloroethylene (TCE) for all optical characterization studies.

Synthesis of Spherical Erucate-Capped PbTe Nanocrystals. The same general procedure for the synthesis of oleate-capped spherical PbTe nanocrystals was followed with the following exceptions and specific reaction conditions. For each reaction in this study, the erucic acid (EA)/oleic acid (OA) ratio was varied from 2.25 EA/0 OA to 0 EA/6 OA, [Pb] = 0.1 M, the injection and growth temperatures were 150 °C and 100 °C, respectively, the lead and tellurium precursors were mixed at a 1:1 ratio, and each reaction was quenched at 4 min with chilled hexane. Since erucic acid is a solid at room temperature, any uncoordinated erucic acid remaining after the reaction that was not removed during the extraction process was removed by centrifuging the NCs in hexane, and then filtering the supernatant through a 0.2 μm PTFE filter.

Synthesis of Cubic-Shaped PbTe Nanocrystals. For this PbTe synthesis, 0.45 g of PbO (2.0 mmol), 2.22 g of technical grade oleic acid (3.5 OA:1Pb ratio), and 15.00 g of technical grade ODE ([Pb] = 0.9 M) were added to a 100 mL round-bottom flask. The mixture was degassed at room temperature for 30 min, and then heated to 193 °C under Ar flow. A volume of 4.0 mL of 0.5 M TOP−Te (2.0 mmol) was rapidly injected into the vigorously stirred reaction vessel. The reaction was terminated by rapidly cooling the reaction vessel. The posttreatment for these PbTe cubic-like NCs was similar to the reported treatment stated above for spherical PbTe NCs except that hexane was added after the vessel had significantly cooled and much less acetone and ethanol were added to crash out these large NCs in the purification process.

Synthesis of Cubic-Shaped PbSe Nanocrystals For synthesizing cubic-like PbSe NCs, 0.45 g of PbO (2.0 mmol), 1.60 g of technical grade oleic acid, and 5.87 g of technical grade ODE were added to a 100 mL round-bottom flask. The mixture was heated to 193 °C under Ar flow for 30 min, and 3.75 mL (∼40 vol %) of the solution was removed. To the remaining, vigorously stirred solution, 1.2 mL of 1 M TOP−Se (1.2 mmol) was rapidly injected. The 3.75 mL portion of the original solution was mixed with 1.5 mL of 1 M TOP−Se and slowly added dropwise from the 4 min mark after the initial injection to the 12 min mark.

Transmission Electron Microscopy (TEM). Transmission electron microscopy (TEM) and high-resolution TEM images of PbTe NCs were taken using a Philips CM 30 operated at 150 or 300 kV, respectively. The self-assembly of PbTe NCs was carried out using amorphous, carbon-coated, copper grids (Ernest F. Fullam Inc. no. 14560) by drop casting a very dilute solution of NCs in 90% hexane/10% octane and allowing the film to assemble and dry in air.

Photoluminescence Quantum Yield Measurements. All spectroscopic measurements shown in this paper were performed on PbTe samples that are as-prepared without any postsynthesis size selection. The room-temperature absorption spectra of PbTe NCs were recorded using a Cary 500 UV−vis−NIR spectrophotometer. Photoluminescence (PL) spectra were measured using a PTI Quantamaster QM 4/2003 steady-state spectrofluorometer equipped with a 600 line/mm grating blazed at 1250 nm on both the excitation and emission sides of the instrument. A steady-state 150 W xenon arc lamp chopped at 28 Hz served as the excitation source, and a Judson liquid nitrogen cooled InGaAs diode detector was used to record the PL. All samples were excited at 890 nm with the entrance and exit slits of the excitation

(30) Reynoso, V. C. S.; Depaula, A. M.; Cuevas, R. F.; Neto, J. A. M.; Alves, O. L.; Cesar, C. L.; Barbosa, L. C. *Electron. Lett.* **1995**, *31*, 1013−1015.
(31) Murray, C. B.; Norris, D. J.; Bawendi, M. G. *J. Am. Chem. Soc.* **1993**, *115*, 8706−8715.
(32) Peng, Z. A.; Peng, X. G. *J. Am. Chem. Soc.* **2001**, *123*, 183−184.
(33) Peng, Z. A.; Peng, X. G. *J. Am. Chem. Soc.* **2002**, *124*, 3343−3353.
(34) Peng, X. G. *Chem. Eur. J.* **2002**, *8*, 335−339.

monochromator fixed at 12 nm spectral resolution. A 10 nm notch-filter centered at 890 nm was placed on the exit slit of the excitation monochromator to reduce the possibility of spurious scattered excitation light. The PbTe NC sample was suspended in TCE and sealed in a Spectrocell 1 cm FUV cuvette under a He atmosphere to prevent photooxidation. The PL emitted at a right angle relative to the excitation source was collected and focused into the emission monochromator. A 1000 nm long-pass filter was placed at the entrance slit of the emission monochromator, and both the entrance and exit slit widths of the emission monochromator were fixed at 7 nm spectral resolution for all measurements. The concentrations of all PbTe samples and the reference dye were adjusted so that the optical densities of all samples were 0.18 ± 0.02 at the excitation wavelength (890 nm), and the small differences in optical densities were taken into account in determining the PLQY. The measurements were carried out 2−4 days after the samples were synthesized. Four PbTe samples having a peak PL intensity ranging between 1150 and 1450 nm were consecutively measured and referenced to the NIR standard dye IR26 (Exciton) in 1,2 dichloroethane.

The dye PL intensity was measured immediately before and after the four PbTe samples, and the difference in the integrated PL intensity of the dye served as a measure of the uncertainty reported in the PLQY. The instrument spectral response was calibrated by observing the spectrum of a precalibrated tungsten−halogen lamp with the InGaAs detector through the collection optics. The quantum yield of the IR26 dye, dissolved in 1, 2 dichloroethane, determined from both absolute and lifetime measurements is reported to be 5×10^{-3}.[35,36] A spectrally calibrated neutral density filter (nominal OD = 2.0) was used to attenuate the PbTe PL to levels comparable to that of the IR26 dye. The absorbance of the filter was recorded between 1 and 1.7 μm and used to correct the PL intensities of the PbTe samples relative to those of the dye.

Multiple Exciton Generation Quantum Yield Measurements. Determination of MEG quantum yields (QYs) via transient absorption (TA) measurements has been described previously.[10,11]

Results and Discussion

Synthesis of Spherical PbTe Nanocrystals. Similarly to the Hines and Scholes'[14] PbS NC synthetic route, we found that when the amount of OA is just sufficient to provide ligand stabilization, the reactivity of the Pb monomer increases. Unlike the PbS synthesis reported, we find that OA/Pb ratios greater than about 12:1 begin to produce NCs with larger size distributions. Also, like the report of Yen et al.[37] on colloidal CdSe NCs, we find that under similar conditions, increasing the amount of anion monomer (TOP−Te) relative to the cation monomer (lead oleate) results in smaller NCs. By decreasing the amount of OA and increasing the amount of injected anion monomer, the number of nuclei formed upon injection increases, which results in smaller NCs because there is less monomer available for the growth phase. For smaller NCs, larger volumes of TOP−Te (approaching a 1:1 Pb/Te ratio) were injected, and the growth temperature, concentration of lead precursor, and OA/Pb ratio were decreased.

Optical Properties of Spherical PbTe Nanocrystals. A range of samples (diluted with TCE such that the first excitonic transition peaks have optical densities between 0.2 and 0.25) demonstrating the tuning of a well-resolved lowest-energy exciton transition from 1009 to 2054 nm is shown in Figure 1a. Figure 1b shows the room-temperature absorption (fwhm = 115 meV) and PL spectra for a sample containing 2.9 nm diameter NCs. The PL peak has a Stokes shift of 65 meV, and a fwhm of 130 meV, indicating that the emission is primarily from the band edge. Relative PLQYs for the four samples measured range between 41 and 52 ± 2%. This result is higher than the 20% PLQY reported for PbS NCs.[14] The relative and absolute PLQY for PbSe NCs in solution has been reported to range from 10% to 85%,[21,23,26] and 6−20%,[9] respectively.

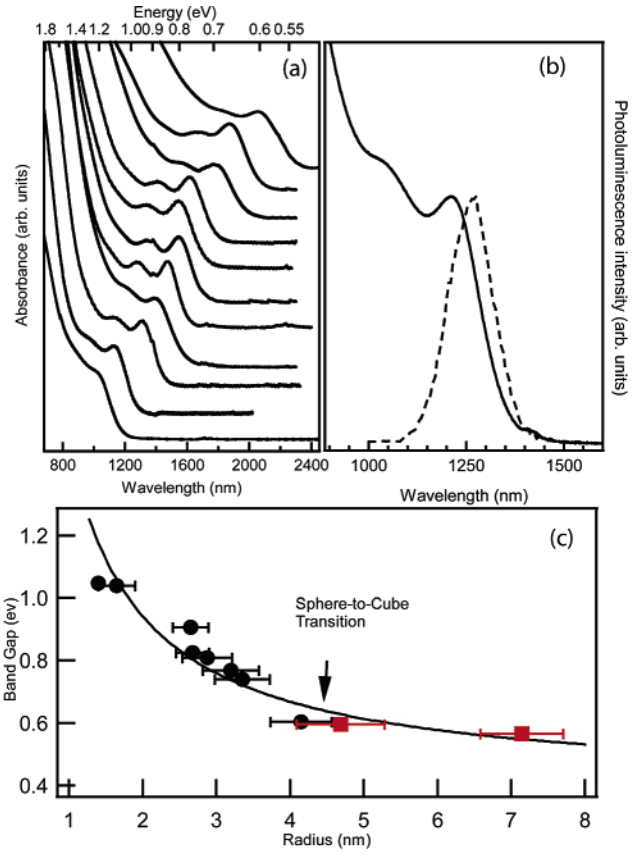

Figure 1. (a) Near-IR spectra of PbTe spherical NCs having a lowest-energy excitonic transition tuned from 1009 to 2054 nm. (b) Linear absorption and PL emission from PbTe NCs having a lowest-energy excitonic transition at 1187 nm and a diameter of 2.9 nm. (c) The radius and shape (circles = spheres, squares = cubes) of PbTe NCs vs the first excitonic transition energy. The bars represent the size distribution of each sample, and the "radius" of cubic NCs is one-half of the edge length. The solid line is a fit to the data of the equation $E(\text{ev}) = b/R - a/R^2 + c$, where R is the radius.

From TEM studies, average diameters of 2.9, 3.3, 5.3, 5.8, 6.4, 6.7, and 8.3 nm were measured for samples having a first excitonic absorption peak centered at wavelengths of 1185, 1194, 1504, 1534, 1614, 1675, and 2054 nm, respectively. Figure 1c shows a plot of the radius and shape of PbTe NCs versus the lowest-energy excitonic transition. The bars attached to each point reflect the size distribution of each sample. TEM measurements of a sample having a first excitonic transition centered at 1534 nm indicate that the relative standard deviation of the size of the PbTe NCs shown in Figure 2, parts a and b, is about 8%. The lattice fringes in the HRTEM image shown in Figure 2b are those of the (200) plane of PbTe. X-ray and wide-angle electron diffraction patterns shown in Figures 2c confirm the highly crystalline rock salt structure of PbTe NCs.

(35) Kopainsky, B.; Qiu, P.; Kaiser, W.; Sens, B.; Drexhage, K. H. *Appl. Phys. B* **1982**, *29*, 15−18.
(36) Seilmeier, A.; Kopainsky, B.; Kaiser, W. *Appl. Phys.* **1980**, *22*, 355−359.
(37) Yen, B. K. H.; Stott, N. E.; Jensen, K. F.; Bawendi, M. G. *Adv. Mater.* **2003**, *15*, 1858−1862.

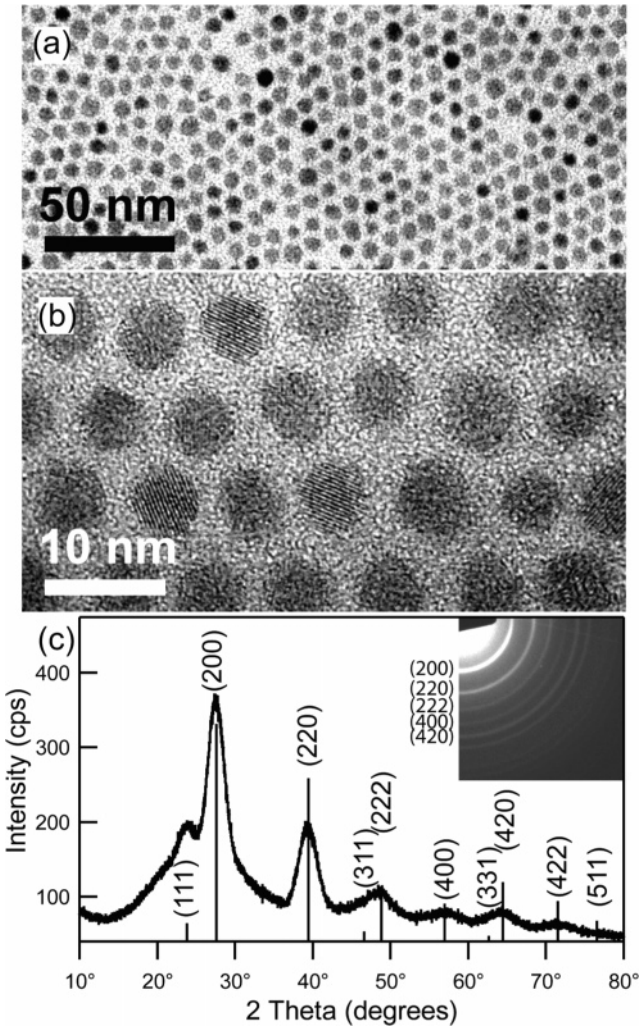

Figure 2. (a) Low-resolution TEM micrograph of an ensemble of the as-prepared PbTe NCs. The PbTe NCs shown here have a lowest-energy excitonic transition at 1534 nm, an average diameter of 5.8 nm, and a size distribution of 8%. (b) High-resolution TEM micrograph of the PbTe NCs from part a in a hexagonal close-packing configuration. (c) XRD pattern of PbTe NCs having a first exciton absorption peak at 1220 nm indexed to the bulk rock salt crystal structure. The NC size calculated from the line broadening of the (220) peak using the Sherrer equation is 2.8 nm. Inset: electron diffractogram of the PbTe NCs with indexing of the main diffraction rings to PbTe.

Cubic-Shaped PbTe Nanocrystals. To further demonstrate the versatility of this PbO one-pot approach for the synthesis of lead chalcogenide NCs,[14,24,26] high-quality, cubic-like, or truncated cubic-shaped[19,38,39] NCs of both PbTe and PbSe have also been synthesized. This report presents alternative routes to the existing synthetic methods to mid-IR-emitting, cubic-shaped PbSe[22] and PbTe[7] NCs. As opposed to spherical PbTe NCs, one round of size selection was used to improve the size distribution. Parts a and b of Figure 3 are TEM images of PbTe NCs from an aliquot removed from the reaction vessel only 10 min after injection. The result is cubic-like PbTe NCs approximately 9.3 nm in size that, for the most part, retain the hexagonal close-packing structure observed in spherical PbTe NCs. The most obvious lattice fringes observed in many of the NCs in Figure 3b were measured and correspond to the (200) planes of the cubic structure of PbTe, having a spacing of 3.23 Å. Figure 3c is a TEM image from an aliquot removed from the vessel at the 15 min mark. These PbTe cubic-like NCs are approximately 14.3 nm in size and adopt a square-packing configuration. Longer growth times produce larger cubic-shaped PbTe NCs. At 35 min, this reaction produced NCs as large as 40 nm that were insoluble in hexane, chloroform, and TCE, even at slightly elevated temperatures. This poor solubility made size selection impossible on these very large NCs that have a poor as-synthesized size distribution. The wide-angle diffraction pattern shown in the inset of Figure 3a and the HRTEM image of Figure 3b reveal that the NCs are highly crystalline PbTe. The small-angle electron diffraction pattern shown in the inset of Figure 3b indicates the formation of a PbTe NC hexagonal array having long-range order.

Cubic-Shaped PbSe Nanocrystals. In addition to injecting TOP−Se instead of TOP−Te, PbSe cubic-like NCs synthesized via this alternative route differ from PbTe in that slow addition of precursor after the initial fast injection produces more uniform cubic-like NCs. As shown in Figure 3d, at 14 min, cubic-like PbSe NCs approximately 15 nm in size are obtained. As with cubic-like PbTe NCs, HRTEM and wide- and small-angle electron diffraction patterns reveal that these PbSe NCs are highly crystalline, rock salt structures that form ordered arrays. Figure 3e shows the as-synthesized mixture of cubic PbSe NCs mixed with smaller NCs (a consequence of Ostwald ripening)[40] that are obtained from this alternative route at a growth time of 20 min. Figure 3f shows an HRTEM image of the cubic-shaped PbSe NCs 27 nm in size that are obtained with a growth time of 20 min.

Shape Evolution. It has been previously reported that lead chalcogenide NCs undergo a shape evolution from spherical/polyhedron to cubic with increasing size.[7,19,22,39,41,42] In our present study of PbTe NCs, we observe highly spherical PbTe NCs as large as 8.3 nm in diameter and near-cubic PbTe NCs having a 9.3 nm edge length. In the only other previous report on synthesizing colloidal PbTe NCs,[7] spherical-shaped NCs were observed at a diameter of ∼8 nm, and near-cubic-shaped NCs were observed having an edge length of ∼14 nm. We find that the actual spherical to cubic transition in PbTe NCs occurs ∼9.3 nm under our reaction conditions. It is interesting to note that Pietryga et al. report,[22] and we confirm using conditions of the same capping ligand and similar temperatures but with using a different cation precursor and solvent, that this transition in morphology does not occur until 13 nm for PbSe NCs. This indicates that changes in the monomer concentration or choice of noncoordinating solvent are not factors in determining the size at which this morphology transition occurs. The NC material composition, growth temperature, and choice of capping ligand are the most important parameters.

Since the PbTe and PbSe NCs reported here were grown under conditions of identical organic ligand and growth temperature, a direct comparison of the size-dependent morphology change observed in these two materials can be made. For rock salt structures, this size-dependent sphere to cube transition is believed to occur in a high-temperature regime, where the higher surface energy {111} face growth in the ⟨111⟩ direction is faster

(38) Wang, Z. L. *J. Phys. Chem. B* **2000**, *104*, 1153−1175.
(39) Jun, Y. W.; Lee, J. H.; Choi, J. S.; Cheon, J. *J. Phys. Chem. B* **2005**, *109*, 14795−14806.
(40) LaMer, V. K.; Dinegar, R. H. *J. Am. Chem. Soc.* **1950**, *72*, 4847−4854.
(41) Lee, S. M.; Cho, S. N.; Cheon, J. *Adv. Mater.* **2003**, *15*, 441−444.
(42) Lu, W. G.; Fang, J. Y.; Ding, Y.; Wang, Z. L. *J. Phys. Chem. B* **2005**, *109*, 19219−19222.

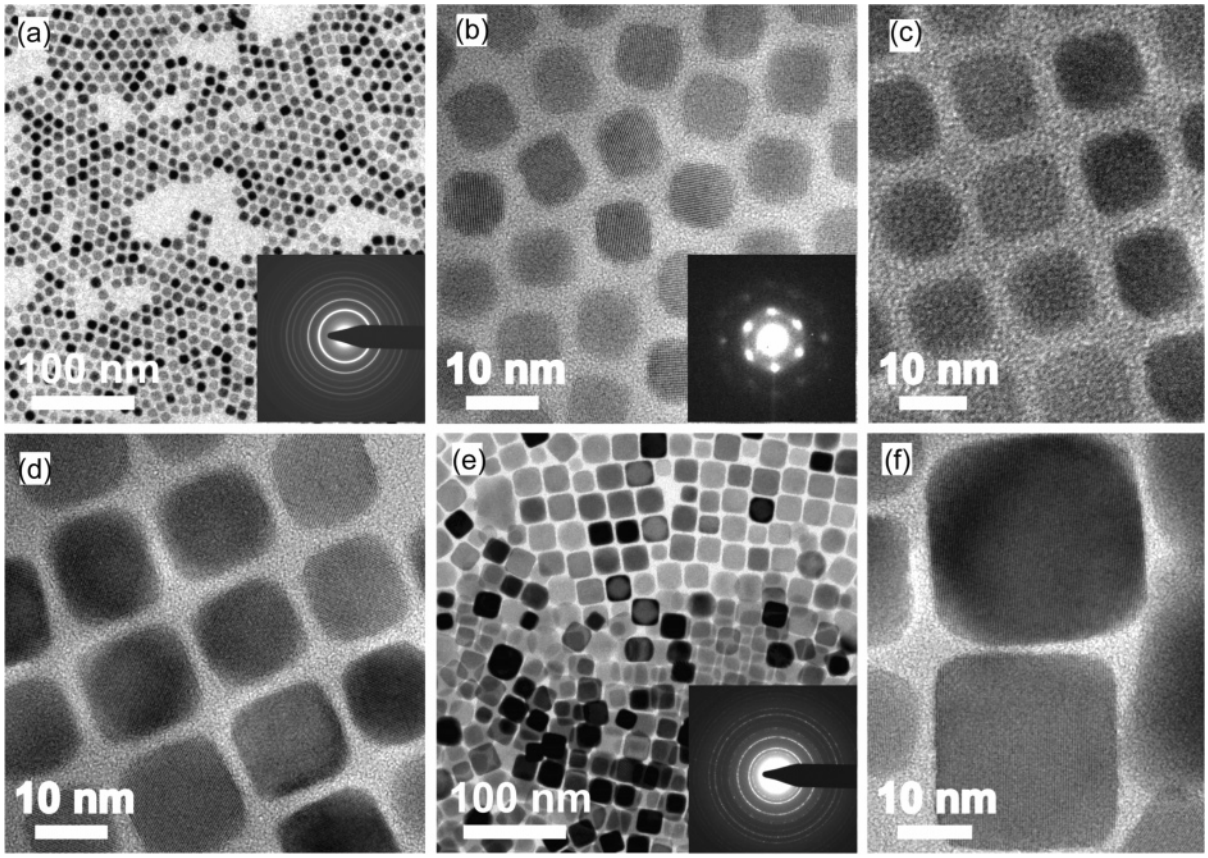

Figure 3. (a) TEM image of as-prepared cubic-like PbTe NCs. (b) The resulting size-selected PbTe NCs undergoing the spherical to cubic transition at 9.3 nm in size. Inset: small-angle electron diffraction pattern from a 1 μm^2 $\{111\}_{SL}$ area. (c) Array consisting of 14.3 nm cubic-shaped PbTe NCs. (d) Ordered array consisting of 15 nm cubic-shaped PbSe NCs after size selection. (e) TEM image of as-synthesized PbSe NCs having a wide size distribution. Inset: wide-angle electron diffraction pattern confirms the highly crystalline rock salt structure of PbSe. (f) HRTEM micrograph of PbSe cubes from part d that are highly crystalline and 27 nm in size.

relative to that of the lower surface energy {100} face growth in the ⟨100⟩ direction.[38,41,43] This favors the growth of the {100} facets leading to a cubic morphology and lowest total surface energy. Thus, since the sphere to cube transition occurs at smaller sizes for PbTe NCs compared to those of PbSe NCs, we conclude that the difference in surface energies between the {111} and {100} faces is greater for PbTe than for PbSe, leading to faster growth in the ⟨111⟩ direction for PbTe and dominance of the {100} faces at smaller NC sizes. Theoretical support for this explanation requires calculations of the surface energies for the {100} and {111} faces in PbTe and PbSe NCs but have not yet been performed.

Tuning the Growth Rate via Ligand Substitution and Concentration. Yu et al.[44] report that the reactivity of the precursor of CdTe semiconducting NCs can be tuned by varying the concentration and type of ligand used to bind to the cation. In addition to using oleic acid, an 18 carbon, monounsaturated carboxylic acid, myristic acid (MA), behenic acid (BA), and erucic acid (EA), were also investigated as possible passivating ligands. Figure 4 shows linear absorption spectra for the erucic acid inquiry which produced the best quality NCs of the three alternative ligands. The only variable that was changed was the EA to OA ratio. Figure 4, spectra a, b, c, and d were from aliquots removed at the 4 min mark containing a ligand-to-lead ratio of 2.25 EA/0 OA/1 Pb, 1 EA/1.25 OA/1 Pb, 0 EA/2.25 OA/1 Pb, and 0 EA/6 OA/1 Pb, respectively. From the blue shift observed in the absorption spectra, it is evident that EA, a 22 carbon monounsaturated carboxylic acid, does indeed

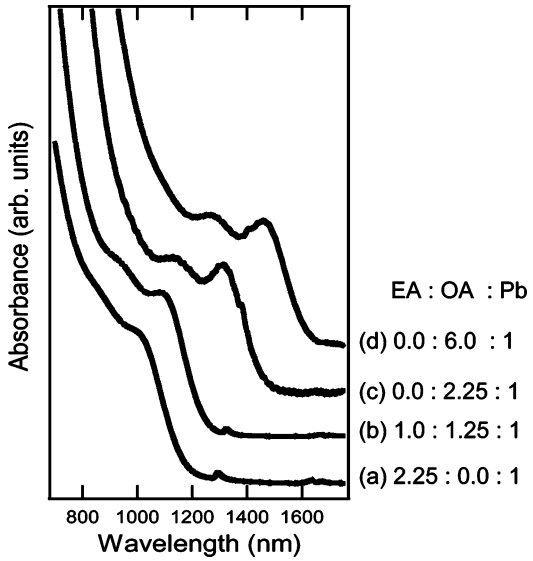

Figure 4. Linear absorption spectra of PbTe NCs containing erucic acid (EA) to oleic acid (OA) to Pb ratios of (a) 2.25 EA/0 OA/1 Pb, (b) 1 EA/1.25 OA/1 Pb, (c) 0 EA/2.25 OA/1 Pb, and (d) 0 EA/6 OA/1 Pb. With this ratio being the only variable in each reaction, tuning of the first excitonic transition occurred from 1006 to 1460 nm.

(43) Jun, Y. W.; Seo, J. W.; Oh, S. J.; Cheon, J. *Coord. Chem. Rev.* **2005**, *249*, 1766−1775.
(44) Yu, W. W.; Wang, Y. A.; Peng, X. G. *Chem. Mater.* **2003**, *15*, 4300−4308.

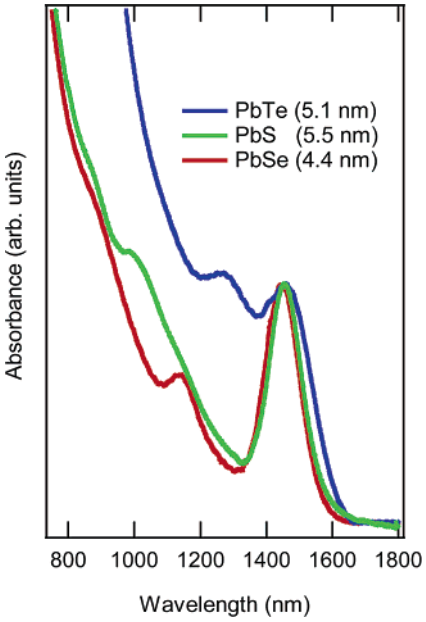

Figure 5. Linear absorption spectra of PbTe, PbSe, and PbS NCs having a first exciton absorption peak at 1450 nm and size distributions less that 10%.

Table 1. Comparison of Lead Salt Properties

lead salt	*R* (nm)	band gap (E_g)	$(E_2 - E_g)/(E_1 - E_g)$	ϵ_∞	a_B ($\perp$)	a_B ($//$)
PbS	5.5	0.41	1.82	17.2	23.5	17.4
PbSe	4.4	0.28	1.4	22.9	66	34.7
PbTe	5.1	0.31	1.23	33	152	12.9

decrease the reactivity of the lead monomer, resulting in smaller NCs. Although size distributions were slightly higher than for oleate-capped NCs, PbTe NCs with EA as the passivating ligand have been synthesized having a first excitonic absorption peak down to 940 nm. Figure 4, spectra c and d, demonstrate that increasing the amount of oleic acid significantly above what is necessary to form the lead oleate precursor results in less nuclei initially forming, thereby leaving larger amounts of monomer available for the growth phase. The net result is that increasing the amount of OA well above the necessary 2 OA/1 Pb ratio produces larger NCs, while substituting a longer passivating ligand for OA produces smaller NCs.

Comparison of Optical Properties of Lead Salt Nanocrystals. Comparing the optical properties of the lead salt nanocrystals may provide insight into their electronic structure and properties. Figure 5 compares the absorption spectra of PbSe and PbTe NCs synthesized in our laboratory with PbS NCs provided by Evident Technologies. All NC colloidal solutions have a first excitonic absorption peak around 1450 nm and size distributions below 10%. The size of the NCs with a first exciton at 1450 nm follows the same pattern as the change in band gap. The bulk band gap is lowest in PbSe and thus to shift the first exciton position to the same value as that of PbTe and PbS a higher degree of confinement is needed; therefore, smaller NCs are required. A list of a few selected properties of the lead salts is found in Table 1. The Bohr radii were computed using parameters from ref 45 and using the equation $a_B = a_0 \epsilon m_e/m^*$ where a_0 is the hydrogen Bohr radius (0.053 nm), ϵ is the high-frequency dielectric constant, and m^* is the reduced effective mass of the exciton ($1/m^* = 1/m_e^* + 1/m_h^*$).

In band structure calculations, spherical constant-energy surfaces inherent in isotropic materials are better represented as ellipsoidal constant-energy surfaces in anisotropic materials.[46−48] We report the longitudinal ($\langle 111 \rangle$ direction) and transverse values of a Bohr ellipse for lead salt NCs in Table 1. The anisotropy becomes more pronounced going down the series: the ratio of the transverse to longitudinal effective mass is ~1.4 for PbS, ~2 for PbSe, and ~12 for PbTe. The anisotropy in PbTe is quite pronounced compared to that of PbS and PbSe. Confinement effects will be felt in PbTe NCs that have a dimension on the 152 nm size scale (compared to 66 nm for PbSe and 23.5 nm for PbS). In fact we are unaware of any crystalline semiconductor with a larger Bohr radius than that of PbTe. It has recently been shown that PbSe nanocrystals can undergo controlled oriented attachment along different crystallographic axes, resulting in NCs with large aspect ratios.[49] The very large longitudinal Bohr radius in PbTe introduces the possibility of synthesizing a high aspect ratio nanomaterial (i.e., elongated shapes) showing quantum-confined effects in three dimensions.

The precise details of how the anisotropy affects the optoelectronic properties in NCs are under investigation. Kang and Wise note that the anisotropy splits the 4-fold degeneracy of the 1S exciton states.[47] We find that the first exciton absorption peak is broader in PbTe compared to that of the PbSe or PbS (see Figure 5). While the PbTe NCs may have a slightly larger size dispersion than the PbSe and PbS samples shown in Figure 5, this cannot account for all of the observed broadening. The broadening is partially due to the large increase in the anisotropy. Although anisotropy affects both low and high exciton states, a recent calculation of the electronic band structure in lead salt NCs found that the anisotropy perturbed the higher-energy states more so than the lowest-energy state.[46] An increase in anisotropy resulted in a spreading out of optical transitions accompanied by a redistribution of the oscillator strengths. We find that the second exciton peak, assigned to the $1S_{h(e)}-1P_{e(h)}$ transition, appears closer in energy to the first exciton peak going from PbS to PbTe. Wehrenberg et al. report a normalized confinement energy for the second exciton peak in PbSe NCs; the confinement energy of the second exciton peak divided by the confinement energy of the first exciton peak.[23] They find that this value remains constant for a given material, independent of the NCs size and temperature; we also find this value to be constant with NC size in PbTe and assume it to be constant in PbS. We report this value in Table 1 for PbS, PbSe, and PbTe. This value decreases going from PbS to PbTe. From simple confinement arguments one would expect the opposite trend, that is, the energy levels should spread out with increasing confinement as is observed in the isotropic calculation of ref 46. However, in the anisotropic calculation from the same reference, this transition is split into a higher- and lower-energy transition. The lower-energy transition resulting from this split

(45) Madelung, O. *Semiconductors: Data Handbook*, 3rd ed.; Springer, Berlin, 2004.
(46) Tudury, G. E.; Marquezini, M. V.; Ferreira, L. G.; Barbosa, L. C.; Cesar, C. L. *Phys. Rev. B* **2000**, *62*, 7357−7364.
(47) Kang, I.; Wise, F. W. *J. Opt. Soc. Am. B* **1997**, *14*, 1632−1646.
(48) Zhang, Y.; Mascarenhas, A.; Jones, E. D. *J. Appl. Phys.* **1998**, *83*, 448−454.
(49) Cho, K. S.; Talapin, D. V.; Gaschler, W.; Murray, C. B. *J. Am. Chem. Soc.* **2005**, *127*, 7140−7147.

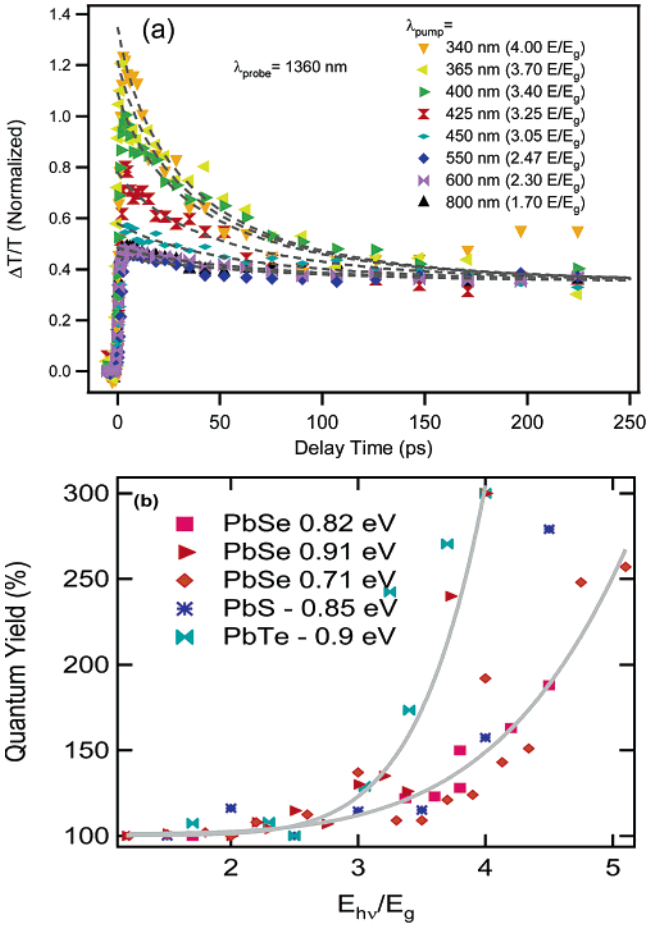

Figure 6. (a) Transient absorption (TA) of PbTe NCs with a first exciton absorption peak at 1360 nm at different pump energies but with constant carrier density, $N_{eh} < 0.5$. The dotted lines are a global fit to the data to extract the MEG QYs. (b) MEG QYs for PbS, PbSe, PbTe; the solid lines are guides to the eye.

is moved closer to the first excitonic transition. This is consistent with observations of PbTe relative to those of PbS and PbSe reported here.

Multiple Exciton Generation. Multiple exciton generation (MEG), recently verified experimentally to be highly efficient in PbSe[10,11] and PbS[11] NCs, is also observed to be very efficient in PbTe NCs. Figure 6a shows the TA dynamics for an increasing excitation energy at a constant excitation density ($N_{eh} < 0.5$). The smooth lines in Figure 6a represent fits to obtain the MEG QYs, based on the fitting procedure described in ref 11 and its appendix. The buildup of multiexciton Auger recombination is readily apparent and indicates efficient MEG. Figure 6b displays MEG QY results for NCs of PbS, PbSe, and PbTe. The solid lines are drawn through two sets of data as guides to the eye. The smallest PbSe NCs and the one size of PbTe NCs have very similar MEG QYs versus $E_{h\nu}/E_g$, while the one size of PbS NCs and two larger PbSe NCs show a slower onset of MEG.

The details of the MEG process in NCs and how its efficiency is affected by various material characteristics are not completely understood. Auger processes, including MEG, are mediated via the Coulomb interaction, and the strength of this interaction in the lead salts should decrease with increasing anion size due to the increasing dielectric constant. On the other hand, the increasing anisotropy with increasing anion size reduces the degeneracy in many of the states, thereby increasing the effective density of states, which should facilitate MEG because more multiexciton states are available to be populated through coupling with highly excited single-exciton states. However, the higher density of states should also facilitate faster cooling, a process which could impede MEG since it is a competitive population relaxation channel that occurs on a similar time scale. Since the MEG QY follows a similar trend with excitation energy as those of PbS and PbSe (Figure 6b), there is no definitive evidence that any of these processes has a dominant effect on the overall QY for MEG. A more complete study of the size-dependent MEG QY in the Pb salts should shed light on these competing processes.

Conclusion

In conclusion, we report a PbO one-pot synthetic method for both spherical and cubic-like relatively monodisperse PbTe NCs (and cubic PbSe NCs) in a noncoordinating solvent. PbTe NCs ranging in size from 2.6 to 18 nm are reported. The spherical NCs are nearly monodisperse, show strong PL emission, and they exhibit highly efficient MEG. Bohr radii for PbS, PbSe, and PbTe are calculated in both the longitudinal and transverse directions to take into account electronic band anisotropy, and a comparison of optical properties of these lead salts is discussed.

Acknowledgment. This work is supported by the U.S. Department of Energy, Office of Science, Office of Basic Energy Sciences, Division of Chemical Sciences, Geosciences, and Biosciences. We thank Evident Technologies for contributing PbS NCs, Dr. Marcus Jones for discussions on photoluminescence quantum yield analysis, and Dr. Yong Zhang for discussions on excitons in anisotropic semiconductors.

JA0574973